University of Groningen

Systematics of Gamow-Teller beta decay "Southeast" of Sn-100

Batist, L.; Gorska, M.; Grawe, H.; Janas, Z.; Kavatsyuk, M.; Karny, M.; Kirchner, R.; La Commara, M.; Mukha, I.; Plochocki, A.

IMPORTANT NOTE: You are advised to consult the publisher's version (publisher's PDF) if you wish to cite from it. Please check the document version below.

Document Version
Publisher's PDF, also known as Version of record

[Link to publication in University of Groningen/UMCG research database](#)

Regular Article – Experimental Physics

Systematics of Gamow-Teller beta decay "Southeast" of ^{100}Sn

L. Batist[1,2,3,a], M. Górska[2], H. Grawe[2], Z. Janas[5], M. Kavatsyuk[4], M. Karny[5], R. Kirchner[2], M. La Commara[6], I. Mukha[2,7], A. Plochocki[5], and E. Roeckl[2]

[1] St. Petersburg Nuclear Physics Institute, RU-188350 Gatchina, Russia
[2] GSI Helmholtzzentrum für Schwerionenforschung, D-64291 Darmstadt, Germany
[3] Max-Planck-Institut für Kernphysik, D-69029 Heidelberg, Germany
[4] KVI, University of Groningen, Zernikelaan 25, NL-9747 AA Groningen, The Netherlands
[5] Institute of Experimental Physics, University of Warsaw, Poland
[6] Department of Physics, University Federico II, and INFN-Napoli, I-80126 Napoli, Italy
[7] IFIC, E-46071 Valencia, Spain

Abstract. The energy centroids and integrated strengths of Gamow-Teller transitions in the β^+ and electron-capture decay are analyzed for nuclei whose proton number Z and neutron number N are restricted to $44 \leq Z \leq 50$ and $50 \leq N \leq 58$. The analysis is based on data measured both with high-resolution γ-ray spectrometry and total γ-ray absorption techniques. The dependence of the considered quantities on the relative neutron excess are established after taking into account the effects due to the Coulomb interaction and mean-field level occupancies. An extrapolation of this dependence to the lightest known tin isotopes is used to estimate the decay characteristics of ^{100}Sn and ^{101}Sn. The values extrapolated for the half-lives of ^{100}Sn and ^{101}Sn agree with experimental data. Using the extrapolated values together with shell model predictions, the Q values for the electron-capture decay of ^{100}Sn is evaluated. The quenching factor for β^+ and the electron-capture decay of the nuclei under consideration here is established to be 0.56(2) with a possible weak dependence on $N - Z$.

1 Introduction

Investigation of β decay remains hitherto the only source of experimental data on spin-charge-exchange excitations in nuclei far from stability. The β^+ and electron-capture (EC) decay in very neutron-deficient nuclei proceeds dominantly by the allowed decay of the Gamow-Teller (GT) type. The decay rate of this disintegration mode is defined by the response to the field

$$g_A/\sqrt{4\pi} \; \sigma t_+, \qquad (1)$$

where σ and t_+ are the spin and isospin operators, $t_+|p\rangle = |n\rangle$, respectively, and g_A is the nucleon axial weak-coupling constant. Summation over nucleons is implicitly included. If the β^+ and/or EC partial intensity (I_β) to individual levels in the daughter nucleus is known, the corresponding reduced probability, $B(\mathrm{GT}_+)$, can be evaluated from the expression

$$B(\mathrm{GT}_+) = 3860 \cdot I_\beta / f t_{1/2}, \qquad (2)$$

a e-mail: batist@pnpi.spb.ru

where $t_{1/2}$ is the half-life of the decaying nucleus. The function f, which takes atomic and lepton phase-space effects into account, is tabulated, *e.g.*, in ref. [1]. The constant $g_A = 1.27 g_V$ is included in the numerical factor given in (2). Thus the reduced probability $B(\mathrm{GT}_+)$ in (2) is defined as

$$B(\mathrm{GT}_+) = ||\sigma t_+||^2/(2J_i + 1). \qquad (3)$$

J_i is the spin of the initial state. Note that the $B(\mathrm{GT}_+)$, evaluated according to (2) and defined in (3), corresponds to the standard definition of the reduced probability of the allowed GT decay [2] and is thus given in units of $g_A^2/4\pi$.

We shall use the symbols B_{GT} for $B(\mathrm{GT}_+)$ strength integrated over the window accessible to EC decay (Q_{EC} window) and $\mathcal{B}_{\mathrm{GT}}$ for the total sum. In case of $\mathcal{B}_{\mathrm{GT}}$ with reference to experiment, it needs some suppositions concerned the strength distribution outside of the experimentally accessible energy region.

Many experiments have shown that the GT strengths observed are much smaller than those predicted by the simple shell model in the independent particle approximation. For taking into account the proton-neutron (PN) correlations which are partly responsible for the suppression

(see, *e.g.*, ref. [3]), the model space has to be complete in the sense that every *l*-orbit is presented by all four of its spin-isospin partners. Calculations of the reduced GT probabilities in the full model space were performed for a series of nuclei in the *p*-, *sd*- and *fp*-shells [4–6]. The suppression of the measured reduced GT probabilities relative to those calculated in the full model space (higher-order suppression [3] or quenching) was found to have a regular character, *i.e.* the ratio between the observed strength and that calculated in the full space is the same for nuclei with the same valence shells. An extension of the analysis to heavier nuclei with inclusion of PN correlations is hindered by the very fast increase of the dimension of the configuration basis.

The present analysis deals with neutron-deficient nuclei whose proton number Z and neutron number N are restricted to $44 \leq Z \leq 50$ and $50 \leq N \leq 58$. In this nuclear region, shell model calculations can be performed in the truncated model space that does not include the proton orbits above the closed shell $Z = 50$. This model space enables one to reproduce the shape of the GT strength distribution. However, the strength cannot be properly normalized because the PN correlations are only partly taken into account, and the value of suppression (reduction factor) does not show a regular behaviour. Therefore, it seems reasonable as a first step to disregard PN correlations and to use, as reference values for the systematics of summed GT$_+$ strengths, an estimate of the bare total strength $\mathcal{B}_{\mathrm{GT}}^{\mathrm{IP}}$ obtained in the independent particle approximation (see *e.g.* ref. [3]),

$$\mathcal{B}_{\mathrm{GT}}^{\mathrm{IP}} = \sum_{j_p, j_n} b_{j_p \to j_n} (2j_p + 1) n_{j_p} (1 - n_{j_n}), \qquad (4)$$

where n_{j_p}, n_{j_n} are the occupancy coefficients of the proton and neutron mean-field orbits j_p and j_n, respectively, and $b_{j_p \to j_n}$ is the reduced probability for the GT transition of one particle from the orbit j_p to the orbit j_n which belong to the same spatial states.

In the nuclear region under consideration, protons partly or completely fill the $g_{9/2}$ orbit. As the neutron $g_{9/2}$ orbit is filled the Pauli principle allows only the spin-flip transformation $\pi g_{9/2} \to \nu g_{7/2}$ which means that summation of (4) is reduced to one term. Note that the (N, Z)-dependence of $\mathcal{B}_{\mathrm{GT}}^{\mathrm{IP}}$ is defined solely by the occupancy coefficients of orbits, which in this case are those with $\pi g_{9/2}$ and $\nu g_{7/2}$ signature. Therefore, provided that the higher-order reduction factor in the region under consideration is approximately constant, the (Z, N)-dependence of the ratio $\mathcal{B}_{\mathrm{GT}}/\mathrm{B}_{\mathrm{GT}}^{\mathrm{IP}}$ (bare reduction factor) is affected by the correlations in the full model space.

The spin-flip transformation of nucleons $j_p \to j_n$ forms the GT$_+$ states in the daughter nucleus. As the neutron excess $(N - Z)$ decreases, the GT$_+$ state, in general being highly fragmented, moves down compared to the parent state. Correspondingly an increasing part of the total strength lies within the Q_{EC} window, thus becoming accessible to the β^+ decay. For very neutron-deficient nuclei the main part of the strength turns out to lie within the Q_{EC} window.

However, the task of a reliable measurement of the strength located at high excitation energy of the daughter nucleus faces a difficulty, the so-called Pandemonium problem [7,8]. The problem concerns the experimental underestimation of the intensity of γ transitions following the β decay to highly excited states of the daughter nucleus. Because of the large density of levels fed by β decay, the β-delayed γ radiation is strongly fragmented. Therefore, a substantial fraction of the intensities of the individual γ transitions may well lie below the sensitivity limit of a detector. The difficulty is even more severe due to the cascade character of the γ de-excitation path. Thus the use of high-resolution (HR) germanium detectors for measuring intensities of individual β-delayed γ-rays and deducing an intensity balance often yields unreliable results, except maybe for the even-even nuclides with their relatively small Q_{EC} values.

A suitable tool for measuring the β-intensity distributions is the total absorption γ spectroscopy [9]. This method uses a large scintillator for γ-ray detection, being characterized by an efficiency close to 100% and an acceptance close to 4π. Such a detector is capable of recording cascades of β-delayed γ-rays rather than single γ transitions, and therefore allows one to restore the entire β-intensity distribution, including weak β transitions to the high-lying excited states in the daughter nucleus.

Making use of the Total Absorption Spectrometer (TAS) [10], the EC and β^+ intensity distributions for some nuclides, "southeast" of ^{100}Sn, including odd and odd-odd ones, have been measured [11–20]. In particular, the TAS data have supplemented experimental results on β^+ decay (here and in following we use a denotation β^+ for both EC and positron emission modes of a decay) that were previously restricted mainly to even-even nuclides. Data obtained with TAS have been partly systematized in ref. [16], where a monotonous isotopic dependence of B_{GT} for the tin isotopes was demonstrated and applied for predicting B_{GT} for ^{100}Sn. In the present analysis we use a considerably extended set of experimental data, including those obtained with the HR technique.

The aim of the present work is to derive approximations characterizing the strength functions of the β^+ decay, namely the energy centroids (see sect. 2.1) and the summed strength (see sect. 2.2) as a function of Z, N. In sect. 2.3 we give an estimate of the higher-order reduction factor of the summed strength for the nuclear region under consideration. This extends the corresponding data derived earlier for the region of *p*-, *sd*- and *fp*-shell nuclei [4–6]. The approximation derived in sect. 2 is used in sect. 3 to extrapolate the systematics to the lightest known tin isotopes, *i.e.* ^{100}Sn and ^{101}Sn. The appendix contains a discussion of previously unpublished TAS results obtained for the β^+ decay of the ground state and a low-spin isomer of ^{100}Ag.

In the following we use the notation "isotopic dependence" for both the proper isotope dependence, *i.e.* the dependence on the mass number of the nuclei under consideration, and for the dependence on the nucleon composition of nuclei with different Z and A, which is expressed

by the asymmetry parameter $I = (N - Z)/A$. The symbol $\mathcal{B}_{\mathrm{GT}}$ without superscript is used for the summed experimental GT_+ strengths, the symbol $\mathcal{B}_{\mathrm{GT}}^{\mathrm{IP}}$ for values estimated by the independent-particle approximation, and the symbol $\mathcal{B}_{\mathrm{GT}}^{\mathrm{FS}}$ for predictions of calculations in the full model space. We would like to specify that the notation "full model space" is used here for the model space which is truncated though, but in which every l-orbit is represented by all four spin-isospin components.

The code OXBASH [21] was used for the shell model calculation supplementing experimental data.

2 Energies and strengths of GT states

Experimental data for the energy centroids and the summed strengths of GT states, measured in the β^+ decay of the nuclides with $44 \leq Z \leq 50$, $50 \leq N \leq 58$ are listed in table 1. Included are data for nuclei whose β^+ decay was investigated with the TAS and/or HR technique. The HR data were accepted here only for even-even nuclei to diminish the above-mentioned problem of a possible loss of β^+ feeding to high-lying states in the daughter nucleus.

As the upper limit of the integration is the Q_{EC} value, the experimental data compiled in table 1 are correspondingly restricted. In accordance with an agreement done in sect. 1 concerning denotations of the reduced probabilities, we use the symbols B_{GT} and E_{GT} for values calculated within the Q_{EC} window, and $\mathcal{B}_{\mathrm{GT}}$ and $\mathcal{E}_{\mathrm{GT}}$ for values which are tentatively obtained without this restriction. The values of B_{GT} presented in table 1 were recalculated from the original data if new values of Q_{EC} have been issued meanwhile. The uncertainties of the integrated strengths, measured by TAS, result from the uncertainties of the Q_{EC} values and from effects owing to insufficient data on the γ-ray branchings [22].

Experimental GT_+ strength distribution for some silver isotopes are displayed in fig. 1 as examples. The figure clearly suggests that almost the whole resonance structure occurs within the Q_{EC} window. In the framework of the shell model these resonances are ascribed to coherent spin-flip $\pi g_{9/2} \rightarrow \nu g_{7/2}$ transformations of paired nucleons, accompanied by pair breaking (seniority change $\delta v = 2$). The corresponding bare GT_+ state in the daughter nucleus can be considered as a particle-hole pair $[\nu g_{7/2} \pi g_{9/2}^{-1}]_{1^+}$ with spin-parity and isospin $S^\pi T = 1^+ 1$, added to the parent state. For even-even parent nuclei this resonance exhausts the GT_+ strength in the Q_{EC} window. In the odd-odd and odd parent nuclei the transformations of the unpaired $g_{9/2}$ proton-particle and/or the unpaired $g_{7/2}$ neutron-hole give rise to components of the strength with $\delta v = 0$, situated below the collective $\delta v = 2$ state. The GT_+ strength of such single-particle transitions is relatively weak, being suppressed by a transfer of the strength to the high-energy resonant structure (see *e.g.* ref. [3]).

Following ref. [23], we define the energy of the GT_+ state, $\mathcal{E}_{\mathrm{GT}}$, with reference to the decaying parent state,

$$\mathcal{E}_{\mathrm{GT}} = \overline{\mathcal{E}}_X - Q_{\mathrm{EC}}, \tag{5}$$

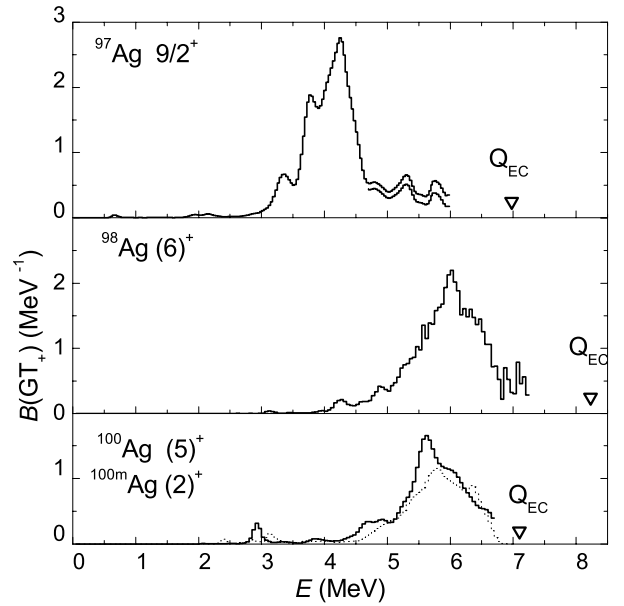**Fig. 1.** GT_+ strength distributions measured with TAS for the decay of ^{97,98,100}Ag. In the upper panel, the region defined by statistical uncertainties for the high-energy tail of distribution for ^{97}Ag is indicated. For the ^{100}Ag decay the distributions for the ground state (solid line histogram) and isomeric state (dotted line histogram) are presented.

where $\overline{\mathcal{E}}_X$ is the centroid of the strength distribution in the daughter nucleus. Correspondingly,

$$E_{\mathrm{GT}} = \overline{E}_X - Q_{\mathrm{EC}}. \tag{6}$$

In order to estimate the possible losses of the integrated strengths and corresponding shifts $\mathcal{E}_{\mathrm{GT}} - E_{\mathrm{GT}}$ we made use of predictions of the many-particle shell model. The OXBASH calculation was performed in the $\pi(p_{1/2}, g_{9/2})$, $\nu(d_{5/2}, g_{7/2}, d_{3/2}, s_{1/2}, h_{11/2})$ model space, with ^{88}Sr taken to be an inert core. The interaction denoted in the following as "96C" [24] was used. Due to computing time restrictions, only 16 values of $E_{\mathrm{GT}}^{\mathrm{SM}}$ and $\mathcal{E}_{\mathrm{GT}}^{\mathrm{SM}}$ were calculated in the nuclear region under consideration here, namely ^{100,101,102,103,104}Sn, ^{100,102}In, ^{98,100}Cd, ^{97,98,99}Ag, ^{96,97,98}Pd, and ^{94}Ru, including the 7 ones investigated with TAS and the 5 ones with the HR technique.

A numerical interrelation between the values of $E_{\mathrm{GT}}^{\mathrm{SM}}$, $\mathcal{E}_{\mathrm{GT}}^{\mathrm{SM}}$ and the ratio $B_{\mathrm{GT}}^{\mathrm{SM}}/\mathcal{B}_{\mathrm{GT}}^{\mathrm{SM}}$ was estimated by using the "averaged" strength distribution shown in fig. 2. This was done by summing the individual strength distributions, each of them being normalized to unity and shifted in energy in order to get all centroids at the same energy. For convenience, the interrelations were approximated by functions of $\mathcal{E}_{\mathrm{GT}}$ that are applicable for $\mathcal{E}_{\mathrm{GT}} < -0.3\,\mathrm{MeV}$

$$
\begin{aligned}
e_q &= \mathcal{E}_{\mathrm{GT}} - E_{\mathrm{GT}} \approx k_1 \cdot \exp(\mathcal{E}_{\mathrm{GT}}/d_1), \\
f_q &= B_{\mathrm{GT}}/\mathcal{B}_{\mathrm{GT}} \approx 1 - k_2 \cdot \exp(\mathcal{E}_{\mathrm{GT}}/d_2),
\end{aligned}
\tag{7}
$$

with $k_1 = 0.6$, $d_1 = 1.12$, and $k_2 = 0.394$, $d_2 = 0.95$.

Applying this to the experimental results, the corresponding distribution averaged over the experimental TAS

Table 1. Integral characteristics of the β^+ decay of nuclei used in the present analysis. Listed are the summed GT_+ strengths B_{GT}, the centroids of the excitation energy of GT_+ distributions $\overline{E}_X$, and the energies of GT_+ states $E_{GT} = \overline{E}_X - Q_{EC}$. Values of Q_{EC} are taken from ref. [25] except for those marked by ^{c}.

Nuclide	B_{GT}	$\overline{E}_X$ (MeV)	E_{GT} (MeV)	Q_{EC} (MeV)
^{108}Sn [26]^a	1.33(5)	0.73	-1.34	2.075(19)
^{106}Sn [27]^a	2.12(20)	1.12	-2.14	3.256(15)^b
^{105}Sn [19]	2.63(35)	3.76	-2.54	6.299(19)^b
^{104}Sn [18]	2.7(3)	1.40	-3.12	4.515(60)
^{103}Sn [17]	3.4(5)	4.11	-3.52	7.635(300)
^{102}Sn [18]	4.2(8)	1.78	-4.00	5.780(70)
^{106}In [13]	1.4(3)	5.43	-1.10	6.526(11)
^{105}In [13]	1.7(2)	3.35	-1.34	4.849(13)
^{104}In [13]	2.1(3)	5.94	-1.84	7.796(8)^b
^{103}In [13]	2.4(3)	3.81	-2.20	6.014(14)^b
^{102}In [15]	4.7(10)	6.41	-2.57	8.968(108)
^{100}In [14]	3.9(9)	6.54	-3.44	10.08(23)
^{102}Cd [28]^a	1.55(16)	0.91	-1.68	2.587(8)
^{100}Cd [29]^a	2.29(26)	1.23	-2.66	3.890(67)
^{98}Cd [30]^a	2.90(22)	1.85	-3.58	5.420(40)
^{100}Ag^c	1.7(2)	5.72	-1.36	7.078(76)
^{100m}Ag^c	1.35(20)	5.75	-1.34	7.093(76)
^{98}Ag [12]	2.7(4)	6.05	-2.19	8.239(63)
^{97}Ag [11]	2.97(40)	4.21	-2.77	6.980(110)
^{98}Pd [31]^a	1.22(12)	0.68	-1.20	1.873(24)
^{96}Pd [32]^a	2.12(16)	1.26	-2.24	3.500(14)
^{94}Ru [33]^a	1.05(15)	0.74	-0.85	1.586(13)

^{a} Measurement performed by means of the high-resolution technique.
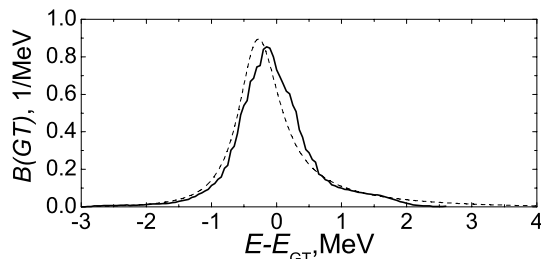^{b} Data evaluated by using data from ref. [34].
^{c} See appendix.

Fig. 2. Averaged normalized strength distributions obtained by summing individual normalized strength distributions from experiment (solid curve) and theoretical OXBASH calculations (dashed curve). The averaged experimental distribution was obtained by using only TAS data. Theoretical data were used according to the list of nuclides presented in the text of sect. 2 with the exception of ^{100}Sn and ^{101}Sn. The resulting distributions were smoothed over energy intervals of 250 keV. The suppression over the high-energy wing of the averaged experimental distribution is connected with the difference between $\mathcal{E}_{GT}$ and E_{GT}.
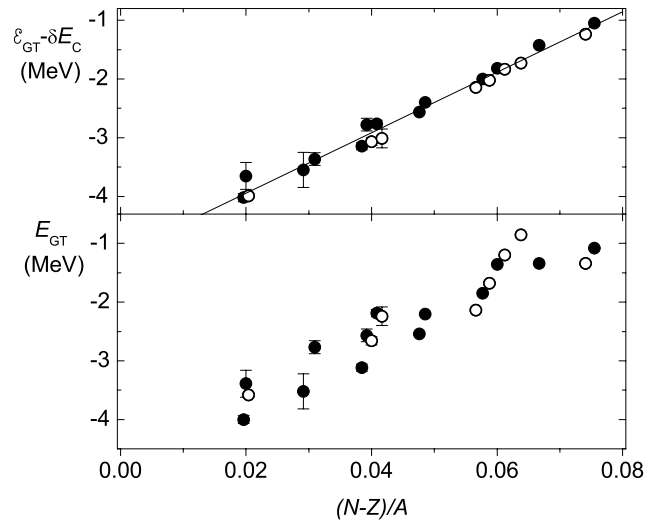
Fig. 3. Isotopic dependence of the average energy of GT_+ states. Filled and empty circles indicate values measured by a total absorption spectrometer and high-resolution germanium detectors, respectively. Uncertainties are only shown if exceeding the size of the data symbols.

data was derived as shown in fig. 2. One can see that a distinction is not so strong to put an interdict on the application of the theoretical interrelation to experiment data.

2.1 Approximation of energies of GT_+ States

The isotopic dependence of the experimental E_{GT} values is shown in the lower panel of fig. 3. The large scattering of the data is mainly due to the Z-dependence of the difference δE_C between the Coulomb energies the daughter and parent nuclei. Taking δE_C into account, the isotopic dependence of $\mathcal{E}_{GT} - \delta E_C$ can be approximated by a linear function of the asymmetry factor $I = (N - Z)/A$ (see the upper panel of fig. 3),

$$\begin{aligned}
\tilde{\mathcal{E}}_{GT} &= a_0 + a_1 \cdot I + \tilde{\delta} E_C \pm e_Z \pm e_N, \\
E_{GT} &\approx \tilde{E}_{GT} = \tilde{\mathcal{E}}_{GT} - e_q.
\end{aligned} \tag{8}$$

Here and in the following, symbols with a tilde sign designate functions that approximate the corresponding variable. The parameters e_Z and e_N were included in the fitting procedure in order to take the dependence on Z and N parities into account, the $\pm$ signs indicating an application to either even or odd numbers of Z and N. The Coulomb staggering was taken in the form

$$\tilde{\delta} E_C = a_C((Z - 1)/A^{1/6} - 49/100^{1/6}). \tag{9}$$

Thus, $\tilde{\delta} E_C$ presents simply a variable part of the Coulomb energy, being scaled so that the correction vanishes for ^{100}Sn. The power of the A-dependence of $\tilde{\delta} E_C$ was taken as $1/6$ in accordance with that of the orbital radius in the oscillator single-particle potential [2]. The parameters

Table 2. Parameters (in MeV) obtained by approximating the experimental and calculated energies of GT$_+$ states by eqs. (8), (9). In the row denoted MSRD, the mean square-root deviations between the experimental and approximating values are presented (see text).

	Experiment	Shell model
a_0	$-4.975(52)$	$-5.280(24)$
a_1	$51.5(10)$	$72.4(10)$
a_C	$-0.512(30)$	$-0.233(22)$
e_N	$-0.011(20)$	$0.061(11)$
e_Z	$-0.078(19)$	$0.017(11)$
MSRD	0.070	0.040

of the approximation (8), (9) obtained by the fit are presented in table 2. The uncertainties of parameters correspond to the one standard deviation. The values of e_q in the second formula of eq. (8) are defined by eq. (7) for an $\mathcal{E}_{GT}$ value calculated according to first formula of eq. (8).

Note that in the upper panel of fig. 3, the symbols corresponding to the $\mathcal{E}_{GT} - \delta E_C$ values obtained by HR measurements systematically lie below the approximating line. This may suggest that the effect is related to a systematic deficiency of the HR method and that the fit can be improved by introducing a correction of the HR data, $E_{GT} \rightarrow E_{GT} + \delta E_{HR}$, with δE_{HR} being the average down-shift of the β-strength functions deduced from HR measurements compared to those from TAS. However, the deficiency of the HR data vanishes if the dependence of the GT$_+$ energy on the Z parity is taken into account. It is important to note that the effect of Z parity remains if only TAS data are fitted. Hence the methodical effect apparent in the HR data is obviously due to the fact that they have been restricted to even-even nuclei. For completeness the N-parity parameter e_N was also included in the fit but the effect turned out to be negligible (see table 2).

The mean square-root deviation (MSRD) between approximating (8), (9) and experimental E_{GT} values amounts to 70 keV. As the uncertainties of the latter data are not well defined, the weights for the fitting procedure were taken from the uncertainties of the corresponding Q_{EC} values unless they were less than MSRD. In the latter case MSRD was assumed for the weights. The average uncertainty in predicting the energies of GT$_+$ states within the interval $0.02 \leq I \leq 0.08$ was estimated to be 90 keV. This result was obtained as a square-root sum of MSRD and a value defined by the matrix of uncertainties of all parameters.

The energies $\mathcal{E}_{GT}^{SM}$ can be approximated by eqs. (8), (9), using the parameters presented in table 2. Both experiment and shell model calculation show a fairly linear isotopic effect. Allowing for a nonlinearity by addition of quadratic and cubic terms in I does not improve the accuracy of the fit.

Note that the Z, N parity effect (parameters e_Z and e_N in table 2) is relatively weak in both the experimental and theoretical GT$_+$ energies. This observation is in agreement with the expectation that the Z, N parity dependence of GT$_+$ energies owing to pairing energy is suppressed because the main component of GT strength is due to transitions with the same change of seniorities, $\delta v_\pi = \delta v_\nu = 1$, independent of the seniority of the decaying state. However, note that parity parameters derived from experimental and theoretical data have the opposite signs. Therefore the experimental parity dependence of GT$_+$ energies cannot be consistently ascribed to an effect of the pairing energy. It should be noted also a quantitative disagreement in the slopes of the isotopic dependencies of GT$_+$ energies and Coulomb corrections, characterized by the parameters a_1 and a_C, respectively (see table 2). This may be connected with a correlation between different parameters, caused by the restricted number of nuclides involved in analysing both experimental and calculated data.

We note that the here applied interaction 96C was adjusted without use of any data on GT distributions. Therefore, the deviations mentioned above might be considered to represent a moderate agreement. In particular, for the group of 12 nuclides for which a direct comparison of calculated and measured GT$_+$ energies is available, the average difference between these quantities was found to be

$$\overline{\delta_E} = \langle E^{SM}(GT) - E(GT) \rangle = 105\,\text{keV},$$

with a mean-square deviation of

$$\langle (E^{SM}(GT) - \overline{\delta_E} - E(GT))^2 \rangle^{1/2} = 210\,\text{keV}.$$

2.2 Approximation of the integral GT$_+$ strength

In order to derive the isotopic dependence of the suppression of the GT strength we took as a reference the values calculated in the independent-particle approach (see eq. (4)). The latter does not include PN correlations. Assuming that the occupancy coefficients n_{j_p}, n_{j_n} for nuclei with $Z \leq 50$, $N \geq 50$ change about linearly with Z and N, eq. (4) can be rewritten as

$$\mathcal{B}_{GT}^{IP} \approx \tilde{\mathcal{B}}_{GT}^{IP} = \frac{160}{9} \frac{Z - Z_0}{50 - Z_0} \frac{N - N_0}{50 - N_0}. \quad (10)$$

The numerical factor 160/9 was obtained by substituting in (4) the values $b_{j_p \rightarrow j_n} = 16/9$ and $(2j_p + 1) = 10$ corresponding to the dominating transformation $\pi g_{9/2} \rightarrow \nu g_{7/2}$. The denominator in (10) implies that at $Z = 50$ the proton occupancy coefficient of the $g_{9/2}$ orbit reaches a value of 1.0, and that there is no blocking of the neutron orbit $g_{7/2}$ at $N = 50$. The parameters Z_0 and N_0 were found from the fit to the occupancy coefficients evaluated from the calculation with Model 96C to be

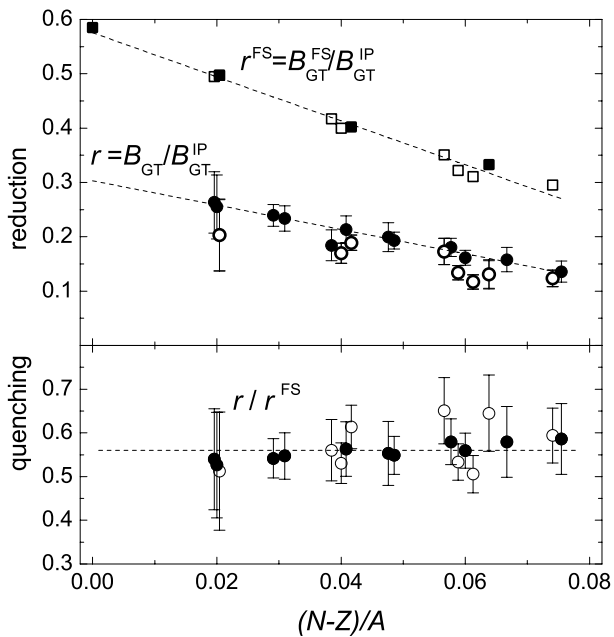$$Z_0 = 39.2, \qquad N_0 = 69.4. \quad (10a)$$

Fig. 4. Upper panel: reduction of the summed experimental (circles) and theoretical (squares) GT_+ strength relative to the prediction of the independent-particle model (10). The experimental $B_{GT}/\mathcal{B}_{GT}^{IP}$ data shown as filled and empty circles stem from TAS and HR experiments, respectively. The theoretical data displayed as filled and empty squares represent results obtained from the SMMC calculation [37,38] and the schematic QRPA calculation, respectively (see sect. 2.3). Lower panel: higher-order reduction factor r/r^{FS} (see sect. 2.3).

The isotopic dependence of the measured summed strength B_{GT} can be seen from fig. 4, where the ratios $B_{GT}/\mathcal{B}_{GT}^{IP}$ are displayed as a function of the $(N-Z)/A$. By taking into account the fraction of total strength situated within the Q_{EC} window, defined by (7), we approximated the isotopic dependence of the reduction factors r by

$$\tilde{r}(I) = r_0 + r_1 \cdot I,$$
$$\tilde{\mathcal{B}}_{GT} = \tilde{r}(I) \cdot \tilde{\mathcal{B}}_{GT}^{IP},$$
$$B_{GT} \approx \tilde{\mathcal{B}}_{GT} \cdot f_q, \qquad (11)$$
$$r_0 = 0.293(11),$$
$$r_1 = -1.72(18).$$

The function $\tilde{r}(I)$ determined from the fit thus approximates the isotopic dependence of the bare reduction factor

$$r = \mathcal{B}_{GT}/\tilde{\mathcal{B}}_{GT}^{IP}. \qquad (12)$$

We have excluded the B_{GT} value of ^{102}In from the fit as it turned out to be about a factor of 1.6, *i.e.* about 3 standard deviations, above the approximating line.

Similar to the observation made for the $\mathcal{E}_{GT}$ values from fig. 3, the symbols corresponding to the reduction factors derived from HR data systematically lie under the smooth approximating line drawn in fig. 4. A corresponding fit shows that the HR data are on average 17(3)%

lower than the TAS data reduced to the same values of I. Moreover, the fit reveals that neither Z nor N numbers parity effects are less than 5%. Therefore, this deficiency of the HR data suggests either a methodical effect or one typical for even-even nuclei to whom the HR data have been restricted. The former explanation does not seem to be convincing since our fit does not detect any noticeable effects of Z and N pairing. The latter interpretation is in agreement with the theoretical estimate of the loss of β-decay strength due to the limited sensitivity of the HR technique [35]. In any case, we conclude that the values of the summed strengths derived from the HR technique are underestimated. In the following treatment, these data were thus taken after dividing them by a factor of 0.83.

With such a correction, (11) provides an accuracy corresponding to an unweighted relative MSRD value of 8%. Taking into account the uncertainty of the parametrization, the accuracy of predicting B_{GT} within the interval of the asymmetry factor I considered is about 9.5%. The weights for the fitting procedure were chosen according to the uncertainties presented in table 1 and were assumed to be 10% for cases where they are below this value. A fitting criterion χ^2 of 0.4 was obtained which indicates that the uncertainties used were overestimated.

The parameter r_1 defines the explicit isotopic dependence of the bare reduction factor. It indicates that the effects of level occupancy and blocking do not exhaust the (Z,N)-dependence of $\mathcal{B}_{GT}$. This property was expected for the suppression of the charge-changing strength. However, the observation of an explicit isotopic dependence contradicts the (Z,N)-dependence that has been established by a previous systematics of the summed $B(GT_+)$ values measured in spin-charge-exchange (n,p) reactions on nuclides of the mid f-shell [36]. In the latter case, an expression $\mathcal{B}_{GT_+} \sim z_{val}(b - n_{val})$ turned out to be sufficient for the description of the (Z,N)-dependence, with z_{val} and n_{val} being the numbers of valence protons and neutrons (see eq. (2) in ref. [36]). In contrast with β^+ decay, the summed GT_+ strength measured in (n,p) reactions is not restricted by the Q_{EC} window. Therefore, though the accuracy of this approximation is not given in ref. [36], the speculation lies close at hand that a supplementary isotopic dependence of the approximation $\mathcal{B}_{GT}$ may have been introduced by an incomplete correction of the undetectable component of the strength that lies at excitation energies above the Q_{EC} window. However, the argument against this suspicion is that a variation of the factor f_q within reasonable limits does not make the parameter r_1 vanish.

2.3 Higher-order reduction

With the aim of dividing the bare reduction factor into the components owing to correlations within and out of the "full model space", we tried to perform a theoretical estimate of the $\mathcal{B}^{FS}$ values (see sect. 1). For this purpose it is necessary to add proton orbits above the magic gap $Z = 50$ to the model space which was used in sect. 2.1 for calculating the isotopic dependence of $\mathcal{E}_{GT}$. A direct

diagonalization in the region of nuclei under consideration is not feasible. Therefore we used the $\mathcal{B}_{\text{GT}}^{\text{FS}}$ values, obtained from the shell model Monte Carlo method (SMMC) in the full oscillator shell $\pi\nu(0g, 1d, 2s)$ [37,38]. The resulting $\mathcal{B}_{\text{GT}}^{\text{FS}}$ values of the $N = 50$ isotones ^{94}Ru, ^{96}Pd, ^{98}Cd and ^{100}Sn are shown in fig. 4 in a manner similar to that used for the corresponding experimental data. Thus we defined the ratios

$$r^{\text{FS}} = \mathcal{B}_{\text{GT}}^{\text{FS}}/\tilde{\mathcal{B}}_{\text{GT}}^{\text{IP}}.$$

In refs. [37,38] the $\mathcal{B}_{\text{GT}}^{\text{FS}}$ values have been presented after being multiplied by a factor $(1/1.26)^2$ which is not included in the data shown in fig. 4. Since the oscillator gds-shell does not include the $2p_{1/2}$ and $0h_{9/2}$ orbits which are part of the space of model $96C$, the parameters Z_0 and N_0 being substituted in (10) were fitted by performing a calculation in the model space $\pi(g_{9/2})$, $\nu(d_{5/2}, g_{7/2}, d_{3/2}, s_{1/2})$.

The four symbols corresponding to the theoretical ratios r^{FS} for isotones with $N = 50$ in fig. 4 can be connected by a straight line. This, however, may be due to the smooth dependence on Z at constant N. In order to further study this effect we estimated the suppression of the summed GT$_+$ strength for some more even-even nuclides in the framework of the schematic QRPA. The calculation were produced in the same model space which was used for the SMMC calculation. The factorized spin-isospin effective interaction was used in both the particle-hole and particle-particle channel. The amplitudes of the interaction were taken as the free parameters and chosen by fitting the summed strength of ^{94}Ru, ^{96}Pd, ^{98}Cd and ^{100}Sn, calculated with QRPA, to the corresponding SMMC values. Note that we do not pretend to describe the core polarization effects in the framework of this approach but merely use it to formally interpolate the SMMC results. The isotopic dependence r^{FS} of the expanded set of nuclides remains to be smooth, and can be approximated, with an accuracy of 3%, by a quadratic function of I,

$$r^{\text{FS}} \approx \tilde{r}^{\text{FS}} = 0.594(16) - 5.54(80)I + 19.4(90)I^2. \quad (13)$$

The reduction factor r^{FS} represents a theoretical estimate of the effect of PN correlation in the space of the main shell $(0g, 1d, 2s)$. Neglecting contributions of the $2p_{1/2}$ and $0h_{11/2}$ orbits to PN correlations, the ratio of experimental reduction, r, to the theoretical one,

$$q = r/\tilde{r}^{\text{FS}} \quad (14)$$

can be considered to yield an estimate of a quenching factor or factor of suppression, caused by the restriction of the model space to the main shell. The q values obtained in this way are displayed in the lower panel of fig. 4. The average value of q for the interval $0.02 \leq (N-Z)/A \leq 0.075$, $\overline{q}$ is 0.56(2), with uncertainty corresponding to the one standard deviation. A formal fit allows for a relative q variation of $(5\pm10)\%$ within the interval $0.02 \leq (N-Z)/A \leq 0.075$. Eliminating the correction f_q decreases the value of the quenching factor by about 6% and forces it on a slightly decreasing slope with increasing I.

Table 3. Properties of ^{100}Sn and ^{101}Sn derived by extrapolating systematics. The uncertainties of the extrapolated E_{GT} and B_{GT} values are estimated by taking into account the uncertainties of the parameters of the approximations and the mean square-root deviations from the approximating functions. The Q_{EC} values are calculated according to (5) as $Q_{\text{EC}} = \overline{E}_X - E_{\text{GT}}$. The uncertainties of Q_{EC} are estimated by taking into account the uncertainties of the extrapolated E_{GT} values and those of the shell model predictions of $\overline{E}_X$, the latter ones being assumed to be about 200 keV.

	^{100}Sn	^{101}Sn	
		$5/2^{+\,a}$	$7/2^{+\,a}$
E_{GT} (MeV)	$-5.065(105)$	$-4.530(90)$	
B_{GT}	$5.21(60)^b$	$4.91(50)$	$4.29(40)$
$t_{1/2}$ (s)^{c,d}	$0.84(17)$	$1.52(35)$	$1.56(35)$
$\overline{E}_X$ (MeV)^e	2.23	4.09	4.39
Q_{EC} (MeV)	$7.29(23)$	$8.62(22)$	$8.92(22)$

^{a} Spin and parity assumed for the ground state.
^{b} Corresponding value $\log ft = 2.87(5)$.
^{c} Calculated using extrapolated E_{GT} and B_{GT} values.
^{d} Experimental $t_{1/2}$ of ^{100}Sn: $0.94_{0.26}^{0.54}$ s [39], $0.55_{0.31}^{0.70}$ s [40]; experimental $t_{1/2}$ of ^{101}Sn: $1.9(3)$ s [17].
^{e} Shell model prediction (see text).

3 Extrapolation to ^{100}Sn and ^{101}Sn

The systematics (8) and (11) can now be used to estimate E_{GT} and B_{GT} values for the lightest known tin isotopes ^{100}Sn and ^{101}Sn. In general, distant extrapolations beyond the interval $0.02 \leq (N-Z)/A \leq 0.075$ to $N = Z$ are ambiguous as an approximating function deduced for a limited interval may fail when applied far beyond it. In particular, the addition of a quadratic on the $(N-Z)/A$ component to the functions approximating the experimental data does not improve the fit but leads to a significant increase of uncertainties of the predictions obtained by extrapolations. Therefore, we estimate the uncertainties stemming from a possible nonlinearity of the approximations by using the corresponding uncertainties which were derived from the fitting of $\mathcal{E}_{\text{GT}}^{\text{SM}}$ and r^{FS}. These values were summed in quadrature to the uncertainties of the prediction which are 90 keV for E_{GT} and 9.5% for B_{GT} (see sects. 2.1 and 2.2). Note that for the isotopes being considered here the corrections according to (7) are negligibly small.

The values of B_{GT} and E_{GT} for ^{100}Sn and ^{101}Sn, obtained by extrapolating the dependences (8) and (11) are listed in table 3. The extrapolated B_{GT} value of $5.21(60)$ for ^{100}Sn can be compared with the value of 5.8 obtained as SMMC prediction [37,38]. The latter one was re-scaled by taking into account the quenching factor $q = 0.56$, evaluated in sect. 2, instead of the factor $(1/1.26)^2 = 0.63$ used in refs. [37,38]. Within the respective uncertainties the extrapolated E_{GT} value of $-5.065(105)$ MeV agrees reasonably well with the experimental estimate of the β end-point energy of ^{100}Sn, *i.e.* $E_{\text{GT}} = -(3.4_{-0.3}^{+0.7} + 1.022)$ MeV [39]. Table 3 contains also

the values of $t_{1/2}$ obtained by using the extrapolated B_{GT} and E_{GT} data obtained in the present work. The Q_{EC} values presented in table 3 were determined according to (5) as $Q_{\mathrm{EC}} = \overline{E}_X - E_{\mathrm{GT}}$, where values of $\overline{E}_X$ were calculated in model 96C.

In the case of the ^{100}Sn decay, only one state with spin and parity 1^+ in the daughter nucleus ^{100}In can be built in the space of model 96C. Therefore, the calculated value of $t_{1/2}$ of this "superallowed" β^+ decay is defined directly by the extrapolated values B_{GT} and E_{GT}. The agreement between the extrapolated $t_{1/2}$ value of ^{100}Sn and the experimental result [39] is satisfactory.

The shell model predicts in ^{101}Sn two low-lying levels with spins and parities $5/2^+$ and $7/2^+$. In the case of the $7/2^+$ assignment, the B_{GT} is suppressed by a factor $7/8$ due to blocking. Moreover, the distribution of the β^+-decay intensity for the ^{101}Sn decay has a nonzero width. Therefore, the $t_{1/2}$ value deduced from B_{GT} and E_{GT} extrapolations depends on the shape of the GT distribution (see discussion in ref. [20]). Therefore, the calculated value of $t_{1/2}$ somewhat depends on which of the two states, either $5/2^+$ or $7/2^+$, is the ground state of ^{101}Sn. The comparison between extrapolated and experimental $t_{1/2}$ of ^{101}Sn (see footnotes in table 3) does not yield a preference for the spin/parity assignment of the ^{101}Sn ground state. Thus this analysis does not allow one to shed light on the conflicting assignments of $5/2^+$ obtained by prompt γ spectroscopy [41] and of $(7/2^+)$ deduced from a ^{105}Te α-decay study [42].

4 Summary and conclusion

The analysis presented here shows that in the region of nuclides where the β^+ decay is dominated by the transformations $\pi g_{9/2} \to \nu g_{7/2}$ the residual isotopic dependence of the energies of GT_+ states and their summed GT reduced probabilities can be approximated by linear functions of the relative neutron excess $(N - Z)/A$. This conclusion is based on the assumption that the effects of Coulomb interaction and the occupancies of single-particle mean-field states are separated. The energy of GT_+ states is fairly well reproduced by the shell model calculation performed in a truncated model space with the interaction 96C.

As far as reduced probabilities are concerned, the deduced isotopic dependence of the GT_+ strength, supplemented to that related to the level occupancies, can be considered to be an experimental manifestation of the effect of nucleon correlations. A comparison of experimental and theoretical reduced probabilities for the β^+ decay of nuclides with $44 \leq Z \leq 50$ and $50 \leq N \leq 58$ leads to the following conclusions: a) the isotopic dependence of the experimental resonance strength is reproduced by a shell model calculation in the full gds model space, and b) the restriction of the basis configurations to the full gds model space leads to the quenching of the GT_+ strength whose value was found to be $q = 0.56(2)$.

This extends the sequence of quenching factors derived from data on the β decay of the p-, sd- and fp-shell nuclei, which were found to be $0.670(22)$ [4], $0.59(3)$ [5] and

$0.554(22)$ [6], respectively. This means that the quenching factors in β decay moderately decrease with increasing shell number.

It is interesting to compare the quenching in β decay with that inherent to the GT resonance excited in spin-charge-exchange reactions on stable target nuclei. In the latter case the quenching factor is defined as $B(\mathrm{GT})$ for the main component of the GT resonance related to the sum-rule strength of $3\,(N - Z)$. In particular, the quenching of the GT resonance in $(^3$He,t) charge-exchange reaction on tin isotopes was found to be $0.63(3)$ [43], which breaks the above-mentioned tendency and differs from the values obtained for β decay of pf- and g-shell nuclei. This indicates that there is probably a relatively weak isotopic dependence of the higher-order reduction of $\mathcal{B}(\mathrm{GT})$ that becomes apparent if one proceeds from neutron-deficient to stable nuclei. This supposition does not contradict the estimate of the isotopic dependence of the higher-order reduction factor derived in this work.

New measurements of decay properties of nuclei near ^{100}Sn which are being planned or have recently been performed (see, *e.g.*, [44]) will hopefully yield improved data and thus shed more light on the physics questions addressed in this paper.

Appendix A. GT_+ strength of ground state and isomer of ^{100}Ag

The GT distribution for the decay of the 2 min, $(5)^+$ ground state of ^{100}Ag was first measured [45] by using a detector with a relatively small sensitive volume which was about five times less than that of TAS. Later-on this decay was reinvestigated with TAS as a by-product during the study of ^{100}In. Beside the decay of the ground state, the decay of the 2.2 min, $(2)^+$ low-spin isomer of ^{100}Ag was investigated. A particular aim of the measurement was to compare the strength functions of the decay of the ground state and isomer.

Heavy-ion reactions mainly feed the ground state rather than the isomer of ^{100}Ag. The mass-separated $A = 100$ beam was purified as described for the $A = 96$ beam in ref. [46]. The isomer ^{100m}Ag was obtained as a daughter from decay of ^{100}Cd. In addition to ^{100g}Cd, the mass-separated $A = 100$ beam in this mode contained an appreciable amount of ^{100g}Ag ions. The decomposition of the registered TAS spectra was necessary to select the spectrum of ^{100m}Ag. For this purpose, we used strong peaks in the TAS spectra that can be reliably related to the decay of the ^{100g}Cd, ^{100}Ag and ^{100m}Ag, respectively. Moreover, the difference in the change of the intensities of theses activities as a function of irradiation/measurement time was used for the decomposition. The ground and

isomeric state have close values of $t_{1/2}$ but the ^{100m}Ag activity contains a component populated by the decay of ^{100}Cd which has a half-life of 40 s. The technique of reconstructing the β^+ and EC intensity distributions was described in detail in ref. [22].

The observation of almost equal energy centroids for the GT$_+$ strengths of ^{100}Ag and ^{100m}Ag is in agreement with TAS data obtained in the rare-earth region [47,48]. This confirms the assumption of a relatively weak effect of unpaired nucleons on the collective GT$_+$ state. The rather significant discrepancy obtained for the B_{GT} values of ^{100}Ag and ^{100m}Ag is most probably due to the poor quality of the data on the latter decay.

References

1. N.B. Gove, M.J. Martin, Nucl. Data Tables A **10**, 205 (1971).
2. A. Bohr, B.R. Mottelson, *Nuclear Structure*, Vol. **1** (Benjamin, New York, 1969).
3. I.S. Towner, Phys. Rep. **155**, 263 (1987).
4. B.H. Wildenthal, M.S. Curtin, B.A. Brown, Phys. Rev. C **28**, 1343 (1983).
5. W.T. Chou, E.K. Warburton, B.A. Brown, Phys. Rev. C **47**, 163 (1993).
6. G. Martínez-Pinedo *et al.*, Phys. Rev. C **53**, R2602 (1996).
7. J.C. Hardy *et al.*, Phys. Lett. B **71**, 307 (1977).
8. J.C. Hardy, B. Jonson, P.G. Hansen, Phys. Lett. B **136**, 331 (1984).
9. C.L. Duke *et al.*, Nucl. Phys. A **151**, 609 (1970).
10. M. Karny *et al.*, Nucl. Instrum. Methods Phys. Res. B **126**, 411 (1997).
11. Z. Hu *et al.*, Phys. Rev. C **60**, 024315 (1999).
12. Z. Hu *et al.*, Phys. Rev. C **62**, 064315 (2000).
13. M. Karny *et al.*, Nucl. Phys. A **690**, 367 (2001).
14. C. Plettner *et al.*, Phys. Rev. C **66**, 044319 (2002).
15. M. Gierlik *et al.*, Nucl. Phys. A **724**, 313 (2003).
16. M. Karny *et al.*, Eur. Phys. J. A **25**, s01, 135 (2005).
17. O. Kavatsyuk *et al.*, Eur. Phys. J. A **25**, s01, 211 (2005).
18. M. Karny *et al.*, Eur. Phys. J. A **27**, 129 (2006).
19. M. Kavatsyuk *et al.*, Eur. Phys. J. A **29**, 183 (2006).
20. O. Kavatsyuk *et al.*, Eur. Phys. J. A **31**, 319 (2007).
21. B.A. Brown *et al.*, MSU-NSCL Report No. 1289 (2004).
22. J.L. Tain, D. Cano-Ott, Nucl. Instrum. Methods Phys. Res. A **571**, 719; 728 (2007).
23. A. Juodagalvis, D.J. Dean, Phys. Rev. C **72**, 024306 (2005).
24. H. Grawe, to be published (2010).
25. G. Audi, O. Bersillon, J. Blachot, A.H. Wapstra, Nucl. Phys. A **729**, 3 (2003).
26. V.P. Burminsky, O.D. Kovrigin, Izv. Akad. Nauk SSSR, Ser. Fiz. **45**, 710 (1981).
27. R. Barden *et al.*, Z. Phys. A **329**, 319 (1988).
28. H. Keller *et al.*, Z. Phys. A **339**, 355 (1991).
29. K. Rykaczewski *et al.*, Z. Phys. A **332**, 275 (1989).
30. A. Płochocki *et al.*, Z. Phys. A **342**, 43 (1992).
31. K. Rykaczewski *et al.*, GSI-90-62 (1990).
32. K. Rykaczewski *et al.*, Z. Phys. A **322**, 263 (1985).
33. E. Eichler, G. Chilosi, N.R. Johnson, Phys. Lett. B **24**, 140 (1967).
34. A. Martin *et al.*, Eur. Phys. J. A **34**, 728 (2007).
35. B.A. Brown, K. Rykaczewski, Phys. Rev. C **50**, R 2270 (1994).
36. S.E. Koonin, K. Langanke, Phys. Lett. B **326**, 5 (1994).
37. D.J. Dean *et al.*, Phys. Lett. B **367**, 17 (1996).
38. S.E. Koonin, D.J. Dean, K. Langanke, Phys. Rep. **278**, 1 (1997).
39. K. Sümmerer *et al.*, Nucl. Phys. A **616**, 341c (1997).
40. D. Bazin *et al.*, Phys. Rev. Lett. **101**, 252501 (2008).
41. D. Seweryniak *et al.*, Phys. Rev. Lett. **99**, 022504 (2007).
42. I.G. Darby *et al.*, contribution to the *5th International Conference on Exotic Nuclei and Atomic Masses (ENAM08), September 7-13, 2008, Ryn, Poland.*
43. K. Pham *et al.*, Phys. Rev. **51**, 426 (1995).
44. T. Faestermann *et al.*, contribution to the *5th International Conference on Exotic Nuclei and Atomic Masses (ENAM08), September 7-13, 2008, Ryn, Poland.*
45. L. Batist *et al.*, Z. Phys. A **351**, 149 (1995).
46. L. Batist *et al.*, Nucl. Phys. A **720**, 245 (2003).
47. A. Algora *et al.*, Phys. Rev. C **68**, 034301 (2003).
48. A. Algora *et al.*, Phys. Rev. C **70**, 064301 (2004).